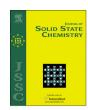
FISEVIER

Contents lists available at ScienceDirect

Journal of Solid State Chemistry

journal homepage: www.elsevier.com/locate/jssc



The electronic structure of the antimony chalcogenide series: Prospects for optoelectronic applications



John J. Carey a, Jeremy P. Allen a, David O. Scanlon b,c, Graeme W. Watson a,*

- ^a School of Chemistry and CRANN, Trinity College Dublin, Dublin 2, Ireland
- ^b University College London, Kathleen Lonsdale Materials Chemistry, 20 Gordon Street, London WC1H 0AJ, United Kingdom
- ^c Diamond Light Source Ltd., Diamond House, Harwell Science and Innovation Campus, Didcot, Oxfordshire OX11 0DE, United Kingdom

ARTICLE INFO

Article history:
Received 21 November 2013
Received in revised form
6 February 2014
Accepted 8 February 2014
Available online 15 February 2014

Keywords:
Antimony chalcogenides
DFT
Electronic structure
Asymmetric density
Band gaps
Solar cell absorbers

ABSTRACT

In this study, density functional theory is used to evaluate the electronic structure of the antimony chalcogenide series. Analysis of the electronic density of states and charge density shows that asymmetric density, or 'lone pairs', forms on the Sb^{III} cations in the distorted oxide, sulphide and selenide materials. The asymmetric density progressively weakens down the series, due to the increase in energy of valence p states from 0 to Te, and is absent for Sb₂Te₃. The fundamental and optical band gaps were calculated and Sb₂O₃, Sb₂S₃ and Sb₂Se₃ have indirect band gaps, while Sb₂Te₃ was calculated to have a direct band gap at Γ . The band gaps are also seen to reduce from Sb₂O₃ to Sb₂Te₃. The optical band gap for Sb₂O₃ makes it a candidate as a transparent conducting oxide, while Sb₂Ss₃ and Sb₂Se₃ have suitable band gaps for thin film solar cell absorbers.

© 2014 Elsevier Inc. All rights reserved.

1. Introduction

The antimony chalcogenides (Sb_2Ch_3 , Ch=O, S, Se, Te) are of considerable interest for optoelectronic applications due to their high refractive indexes, photo-sensitivity, high electrical conductivity, strong adsorption and transport properties [1-14]. Antimony oxide (Sb₂O₃) is a potential candidate for photocatalysis due to its large and direct band gap located in the near-ultraviolet region [1,2]. Sb₂O₃ is useful as a flame-retardant in polymers, adhesives and textile back coatings [15-17]. Antimony sulphide (Sb₂S₃) has potential applications in solar energy conversion [11], thermoelectrics and optoelectronics [10,12] while antimony selenide (Sb₂Se₃), a high refractive material, is used for optical coatings in thermophotovoltaic applications [18], optical storage and photovoltaic conversion [19]. Antimony telluride (Sb₂Te₃) is mainly used as a thermoelectric material [20-23] and has recently been identified as a topological insulator (TI), which contains an insulating bulk band gap and gapless metallic surface conductivity [24,25].

The Sb₂O₃ structure exists in three different polymorphs (α, β) and γ) with each being distorted from the presence of lone pairs on the Sb^{III} cations [26]. The focus of previous studies for Sb₂O₃ has been the electrical, vibrational and optical properties [6,7,27–29].

Optical band gaps in the range of 3.40–4.00 eV have been reported for Sb₂O₃, with the indirect/direct nature of the band gap unclear [6,7,28]. Hartree-Fock calculations were used to characterise the electronic density of the Sb₄O₆ clusters in the senarmontite structure, indicating the presence of lone pairs on the Sb cations [30]. The ground state vibrational frequencies and molecular orbitals were deduced using second order Møller-Plesset and density functional theory (DFT) using the B3LYP exchange correlation functional [27]; however, there was no examination of lone pairs or band structure analysis. A DFT study by Matsumoto et al. [31] using the Perdew-Burke-Ernzerhof (PBE) exchange correlation functional based on the generalised gradient approximation (GGA) examined the ground state electronic structure of Sb₂O₃, along with As₂O₃ and Bi₂O₃. The electronic band structure for Sb₂O₃ was examined, calculating a fundamental band gap of 3.33 eV; however, neither the direct/indirect nature of the fundamental band gap nor optical adsorption was investigated. Band structure calculations for Sb₂S₃ using PBE-DFT show that it possesses an indirect fundamental band gap of 1.35 eV with the valence band maximum and conduction band minimum located at Γ and Y, respectively [32]. Sb₂S₃ has a direct optical band gap with experimental studies reporting a range from 1.66 to 2.24 eV [14,32-41], which is found to increase with the film thickness and temperature [42,43]. The nature of the band gap for Sb₂Se₃ is also unclear but an experimental range of 1.00-1.82 eV has been reported, where the lower energy transitions are considered to be indirect [44-47]. A PBE

^{*} Corresponding author.

E-mail address: watsong@tcd.ie (G.W. Watson).

study by Vadapoo et al. [48] calculated an indirect band gap of 0.88 eV for Sb₂Se₃; however this is likely to be an underestimated value which is often the case when using a GGA functional like PBE. The optical band gap for Sb₂Te₃ has been investigated experimentally with values between 0.29 eV and 0.46 eV depending on film thickness [49,50]; however the indirect/direct nature of the transitions was not ascertained. For Sb₂Te₃, theoretical studies have focused on explaining the thermoelectric properties and the effect of uniaxial pressure on its band structure [20,21,51,52]. The calculated band structure of Sb₂Te₃ is in contention as some reports have shown that it is a direct band gap material at Γ (0.14 eV) [53], while others have indicated that its VBM and CBM are off set from the high symmetry points in the Z-F and Γ –Z directions, respectively, with a band gap of 0.28 eV [20,21,54]. Thonhauser et al. [52] suggested that this discrepancy is a result of the presence or absence of spin orbit coupling (SOC) with the VBM located in the Z–F direction with SOC and at Γ without; however, Park et al. [23] suggested that the difference in the position of the VBM/CBM is related to the change in the volume of the relaxed cell with SOC leading to a reduction in the volume relative to PBE.

The atomic structures of antimony oxide, sulphide and selenide are all distorted, while the telluride adopts a highly symmetric hexagonal structure. The crystal distortion and the stabilisation of these materials are typically explained by the presence of Sb^{III} 'lone pairs' [26,30]. The electronic structure of the Sb^{III} cation is [Kr] $4d^{10}5s^25p^0$, where the 5s electrons are thought to form a chemically inactive sp hybridised lone pair [55,56] which is sterically active, resulting in a distorted coordination environment for the Sb^{III} cation. The same argument, however, would also predict Sb₂Te₃ to possess a distorted structure. The lack of distortion suggests that the role of lone pairs in these crystal structures is more complicated than previously described.

The inert pair effect [57] was originally challenged by Watson and Parker using DFT and the PW91 functional to calculate the electronic structure of α -PbO [58,59]. They showed that the classical sp hybrid orbital cannot form as the energy gap between the 6s and 6p orbitals is too large. The distorted α -PbO structure was found to arise from the stabilisation of the anti-bonding Pb(6s)-O(2p) interaction at the top of the valence band by the Pb 6p states. This theory was later supported by experimental studies [60,61].

As the formation of the lone pair was found to be dependent on the interaction of the cation with the O 2p states, the effect of changing the anion on the lone pair was further investigated by Walsh and Watson for PbO and PbS and the Sn monochalcogenide series [62,63]. From PbO to PbS, as well as moving down the Sn monochalcogenides, the structure progresses from a distorted litharge structure to the symmetric rocksalt motif. In both instances, the distorted structures are found to contain asymmetric charge density (lone pairs) on the cations, which are absent in the symmetric structures. The change in lone pair activity was shown to be a result of the energy gap between the cation s states and the anion p states increasing from the oxide (2p) to the telluride (5p). The revised model has since been extended to other lone pair materials such as SnO [64,65], Bi₂O₃ [66], Bi₂Sn₂O₇ [67], Pb₂MgWO₆ [68], BiMnO₃ [69], BiOF, Bi₂Ti₂O₇ [70], and Bi₂Tc₂O₇ $-\delta$ [71]. A recent study by Matsumoto et al. [31] supported the role of the anion in the formation of the lone pairs, and the stabilisation of the Sb₂O₃, As₂O₃ and Bi₂O₃ distorted structures.

The formation of lone pairs in such materials leads to a mixed valence band of metal s/p and anion p states. The extent of mixing between the metal s and anion p states creates a dispersed valence band with the VBM raised through the anti-bonding nature of the interactions. This can reduce the band gap and has become an important concept in band gap engineering and is used to design

devices with tailored band gaps for optoelectronic applications [72–75]. Additionally, the valence band mixing of metal *s* with anion *p* states suggests that materials with lone pairs on the cations may be good candidates for *p*-type conducting materials [76–79]. As the Sb^{III} cations are expected to possess lone pairs for the distorted systems, this may indicate that they could be potential candidates for *p*-type conducting materials. Furthermore, altering the anion from O to Se may reduce the band gap and improve their properties for optoelectronic devices [7,12].

As previous studies [30,36] have attributed the lone pair formation to the classical sp hybrid orbital description, rather than a stabilisation of Sb–Ch antibonding orbitals, the electronic structure of the antimony chalcogenides will need to be re-examined as described by the revised model [58]. This study will thus examine the electronic structure of the antimony chalcogenide series using DFT calculations employing the PBE functional. Electronic density of states (EDOS), partial (ion and l-quantum number decomposed) density of states (PEDOS) and charge density plots are used to provide a full characterisation of the Sb_2Ch_3 bonding characteristics, identifying any trends across the series.

2. Theory/calculation

Periodic-DFT was used through the VASP code [80,81] with a plane wave basis set. The interactions between the core (Sb:[Kr]4d¹⁰, O:[He], S:[Ne], Se:[Ar]3d¹⁰, Te:[Kr]4d¹⁰) and valence electrons were described using the projector-augmented wave (PAW) approach [82]. All calculations were performed using the PBE [83] exchange-correlation functional.

Optimisation of the structures was performed through a series of constant volume calculations, where the lattice vectors, angles and atomic positions were allowed to relax while the cell volume was kept constant. The energies obtained were fitted to the Murnaghan equation of state [84] to find the minimum energy volume. This approach minimises potential problems of Pulay stress and changes in basis set which can accompany volume changes in plane wave calculations. Although the Pulay stress can be anisotropic, this method has been shown to be accurate by comparing the pressure along different lattice vectors for the SnO structure with 500 eV and 1000 eV cut-offs [85]. Primitive cells were used for each system and the structures were deemed converged when the force on each ion was less than 0.01 eV/Å. An energy cut-off parameter of 500 eV and a Monkhorst-Pack [86] *k*-point sampling grid of $6 \times 6 \times 6$ for Sb_2O_3 , $2 \times 12 \times 2$ for Sb_2S_3 , $2 \times 2 \times 12$ for Sb_2Se_3 and $6 \times 6 \times 2$ for Sb_2Te_3 were sufficient for convergence. To calculate the PEDOS, the wavefunctions were projected onto spherical harmonics centred on each atom with a radius of 1.45, 1.55, 1.88, 2.05, 2.07 Å for Sb, O, S, Se and Te, respectively. For Sb₂Se₃ and Sb₂Te₃, spin-orbit coupling was included to asses its effect on orbital contributions to the top of the valence band (VB) and the bottom of the conduction band (CB), since this is required for DFT studies of TIs [87].

The optical absorption spectra and the optical transition matrices were calculated within the transversal approximation [88]. The Tauc relation states that for a direct allowed transition, the optical band gap of a material can be obtained by plotting $(\alpha h \nu)^2$ versus $h \nu$ and extrapolating $(\alpha h \nu)^2$ to zero, as described previously [89]. This approach sums all direct VB to CB transitions on the k-point grid but does not take into account indirect and intraband transitions [90]. Single-particle transitions are only considered, thus electron–hole correlations are not treated and would require higher order electronic structure methods [91–93]. The approach has been shown to provide reasonable optical absorption spectra in comparison to experiment [94–97,89].

Download English Version:

https://daneshyari.com/en/article/7759260

Download Persian Version:

https://daneshyari.com/article/7759260

<u>Daneshyari.com</u>